CONF-831047--22

FINAL

STRUCTURE OF HIGH-BURNUP-FUEL ZIRCALOY CLADDING*

H. M. Chung

Materials Science and Technology Division
Argonne National Laboratory
Argonne, Illinois 60439

June 1983

CONF-831047--22

DE83 014699

To be submitted to the American Nuclear Society Winter Meeting, October 30-November 4, 1983, San Francisco, CA.

*Work supported by the Office of Nuclear Regulatory Research, U. S. Nuclear Regulatory Commission.

STRUCTURE OF HIGH-BURNUP-FUEL ZIRCALOY CLADDING*

H. M. Chung

Materials Science and Technology Division
Argonne National Laboratory
Argonne, Illinois 60439

SUMMARY

Zircaloy cladding from high-burnup (>20 MWd/kg U) fuel rods in light-water reactors is characterized by a high density of irradiation-induced defects (RID), compositional changes (e.g., oxygen and hydrogen uptake) associated with in-service corrosion, and geometrical changes produced by creepdown, bowing, and irradiation-induced growth. During a reactor power transient, the cladding is subject to localized stress imposed by thermal expansion of the cracked fuel pellets and to mechanical constraints imposed by pellet-cladding friction. The material with high-density RIDs is conducive to deformation by dislocation channeling rather than by normal prismatic slip resulting in irradiation-induced embrittlement. Besides the irradiation embrittlement, the deformation and fracture of the high-burnup fuel cladding may be influenced by other synergistic factors, e.g., strain aging (an interaction between stress and impurity elements), which is most pronounced at ~325°C for oxygen atoms,[1,2] irradiation-induced segregation of alloying or impurity atoms[3-5] (interaction between RID and nonmatrix elements), and the formation of nonequilibrium phases under irradiation.[6] As part of a program to provide a better understanding of brittle-type failure of Zircaloy fuel cladding by pellet-cladding interaction (PCI) phenomenon, the stress-rupture properties and microstructural characteristics of high-burnup spent fuel

*Work supported by the Office of Nuclear Regulatory Research, U. S. Nuclear Regulatory Commission.

cladding have been under investigation.[7,8] This paper reports the results of the microstructural examinations by optical microscopy, scanning (SEM), 100-keV transmission (TEM), and 1 MeV high-voltage (HVEM) electron microscopies of the fractured spent fuel cladding with a specific emphasis on a correlation of the structural characteristics with the fracture behavior.

The cladding tubes irradiated to high burnup in the Big Rock Point or H. B. Robinson reactor were deformed to fracture by gas-pressurization loading at 292-325°C, in which the inner- and outer-surface was exposed to research-grade helium or argon without any fission-product simulants. SEM examination revealed pseudocleavage-plus-fluting features, characteristic of a PCI-type fracture surface, in 6 out of 11 test specimens. Metallographic cross sections of the failure regions of the six specimens were also characterized by small diametral strains ($\lesssim$1%) and numerous branching cracks.

TEM-HVEM evaluations of thin foil specimens obtained from regions adjacent to the failure sites revealed that the brittle-type fracture was characterized by lack of slip dislocations and numerous locations that contained an extensive amount of second-phase precipitates. The precipitate particles were ellipsoidal in morphology with a size of 100-200 Å [see Fig. 1(A)], and observed primarily in cell wall regions as dense aggregates in association with dislocation substructures. From analyses of diffraction characteristics, the precipitate was identified as the ordered zirconium-oxygen phase of Zr_3O,[9] which is known to be metallic and of brittle character.[10] Diffraction patterns from regions containing Zr_3O phase are characterized by numerous double diffraction spots or weak superlattice reflections due to the ordered occupation of octahedral sites in the α-matrix by oxygen atoms. In this regard, examination of thick regions of the foil specimen by HVEM proved to be most advantageous for the analysis of Zr_3O.

To provide a more quantitative correlation between the brittle-type fracture and distribution of Zr_3O precipitates, it was necessary to show the distribution of dark-field images of the characteristic superlattice reflections. To facilitate the method, orientational relationships between the α-Zr matrix and Zr_3O phase were determined. Figure 1(A) shows a bright-field image of a selected area of a thin foil specimen excised from a region adjacent to a brittle-type failure site that exhibited pseudocleavage-plus-fluting features over a large portion of the fracture surface. Aggregates of small Zr_3O precipitates (dark regions) can be observed in association with weak contrasts from dislocations. As shown in the indexed diffraction pattern of Fig. 1(B), the selected area also contains χ-hydrides which have been shown to be an artifact surface phase.[7]

The $(51\bar{6}1)_s$, $(21\bar{3}2)_s$, $(\bar{2}1\bar{3}\bar{2})_s$, and $(4\bar{1}\bar{3}4)_s$ reflections of the Zr_3O phase in Fig. 1(B) are the characteristic superlattice spots, produced from the ordered oxygen atoms only. For these reflections, the wave amplitudes scattered from Zr atoms are extinct. The indexed diffraction pattern of Fig. 1(B) shows the zone axes $[\bar{1}0\ 17\ \bar{7}\ \bar{9}]_{Zr_3O}$ // $[\bar{4}\ 5\ \bar{1}\ \bar{1}5]_\alpha$ and planes $(21\bar{3}2)_{Zr_3O}$ // $(\bar{1}2\bar{1}1)_\alpha$. Similar diffraction analyses from other regions showed orientations of Zr_3O precipitates equivalent to that of Fig. 1(B).[8] This kind of orientation can be denoted as $(0001)_{Zr_3O}$ // $(10\bar{1}0)_\alpha$ and $[\bar{1}2\bar{1}0]_{Zr_3O}$ // $[0001]_\alpha$. The indexed diffraction pattern shown in Fig. 2(A) corresponds to an orientation of a different kind, i.e., zone axes $[32\bar{1}\bar{3}]_{Zr_3O}$ // $[11\bar{4}\bar{7}6]_\alpha$ and planes $(2\bar{1}\bar{2}3)_{Zr_3O}$ // $(10\bar{1}3)_\alpha$. Orientations equivalent to Fig. 2(A) were also observed from numerous selected area diffraction patterns.[8] This kind of orientation can be denoted as $(0001)_{Zr_3O}$ // $(0001)_\alpha$ and $[2\bar{1}\bar{1}0]_{Zr_3O}$ // $[10\bar{1}0]_\alpha$. This orientational relationship is identical to that reported by Holmberg and Dagerhamn[9] from

x-ray diffraction analysis. Figure 2(B) is a negative contrast of the dark-field image of $(11\bar{2}1)_{Zr_3O}$ of Fig. 1(E), which shows a distribution of Zr_3O particles. The diffraction pattern of Fig. 2(A) was obtained from the selected area denoted by a circle in Fig. 2(B).

From the results of the microstructural examinations reported here, it appears that the brittle-type failures are associated with segregation of oxygen atoms in the stress-concentrated region, which subsequently led to the formation of the Zr_3O phase and an immobilization of dislocations. On the basis of evidence for oxygen segregation by a strain-aging phenomenon at ~325°C in Zr-O alloys,[1,2] as well as irradiation-induced segregation of oxygen in Nb-O[3] and V-O alloys,[4,5] it appears to be entirely possible that the precipitation of the Zr_3O phase in the high-burnup spent fuel cladding could be enhanced by the simultaneous presence of high-density irradiation-induced defects, and repeated local stresses imposed by the expanding UO_2 pellets during power cycling. Under such a nonequilibrium situation, the structure of Zircaloy fuel cladding, a material no longer similar to that of the originally fabricated state, appears to be susceptible to a brittle-type failure.

References

1. P. M. Kelly and P. D. Smith, J. Nucl. Mater. 46, 23 (1973).

2. W. R. Thorpe and I. O. Smith, J. Nucl. Mater. 80, 35 (1979).

3. J. M. Williams, W. E. Brundage, and J. T. Stanley, Met. Sci. J. 2, 100 (1968).

4. N. Igata, K. Miyahara, K. Ohno, and K. Hakomori, J. Nucl. Mater. 108&109, 239 (1982).

5. R. P. Agarwala, B. M. Pande, and M. S. Anand, ibid., p. 240.

6. "Phase Transformation During Irradiation," Elsevier Science Publishing Company, 1983, Ed. F. V. Nolfi.

7. Materials Science Division Light-Water Reactor Safety Research Program: Quarterly Progress Report, July-September 1982, NUREG/CR-2970 Vol. III, ANL-82-41 Vol. III, Argonne National Laboratory.

8. ibid., October-December 1982, Vol. IV.

9. B. Holmberg and T. Dagerhamn, Acta Chem. Scand. 15, 919 (1961).

10. P. Lehr and J. Debuigne, Sixth Collogue de Métallurgie, North Holland Publishing Company, Amsterdam, Netherlands (1963), p. 139.

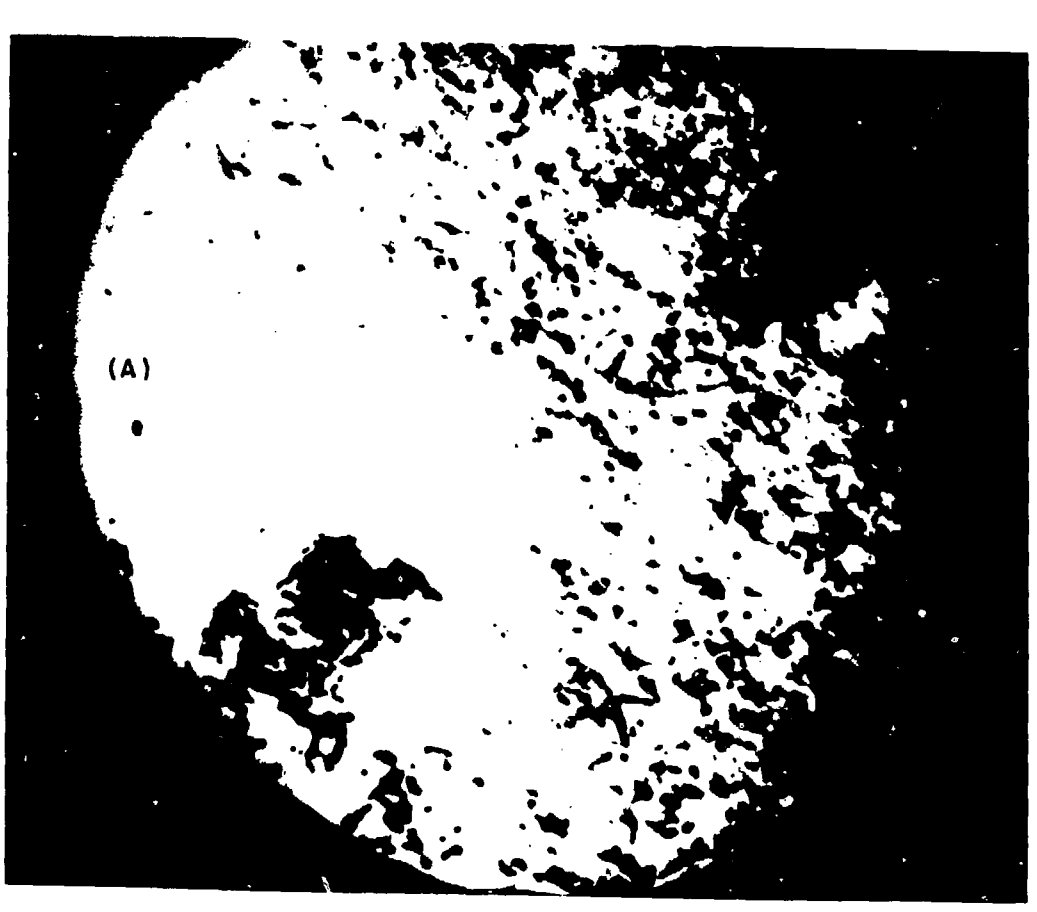

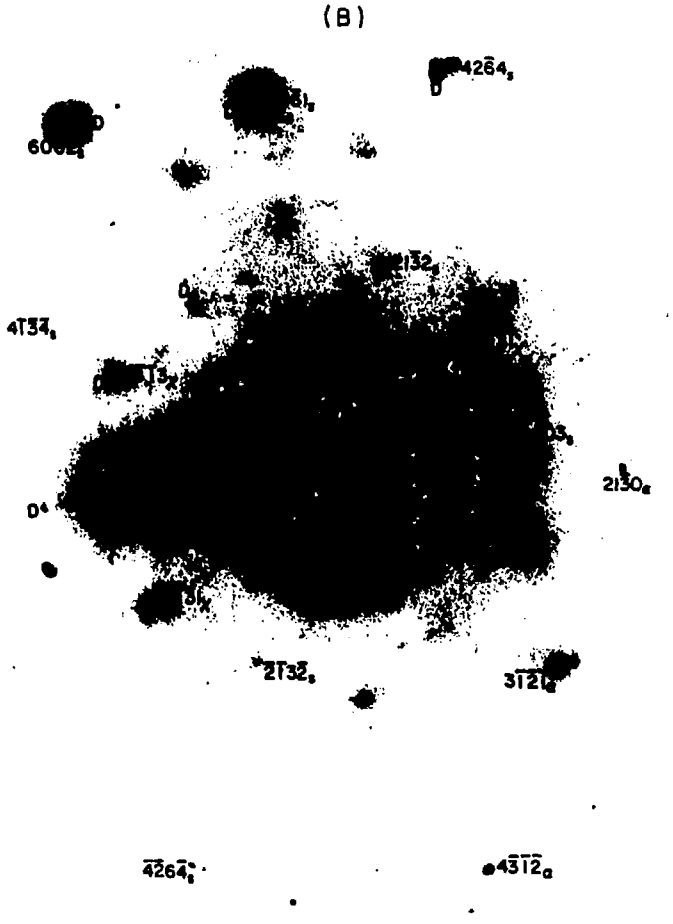

Fig. 1. 100 keV-TEM microstructure of a thin foil specimen from Big Rock Point spent fuel cladding containing Zr_3O precipitates. (A) Bright-field morphology; (B) selected area diffraction pattern of (A), showing Zr_3O-phase superlattice reflections and zone axes $[\bar{1}\bar{0}\ 17\ \bar{7}\ \bar{9}]_{Zr_3O}$ // $[\bar{4}\ 5\ \bar{1}\ \bar{1}\bar{5}]_{\alpha}$ and planes $(21\bar{3}2)_{Zr_3O}$ // $(\bar{1}2\bar{1}1)_{\alpha}$.

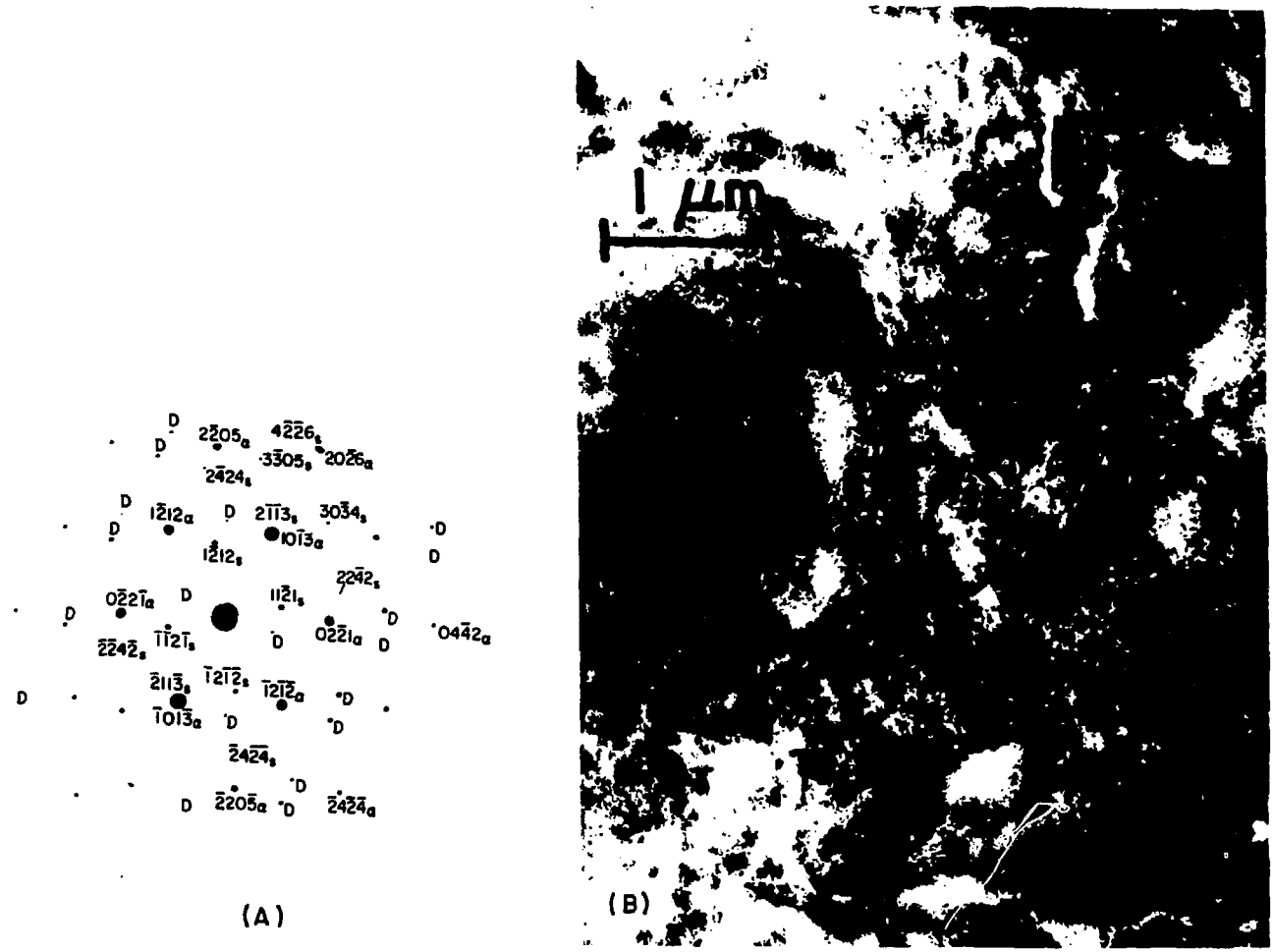

Fig. 2. 1 MeV-HVEM microstructures of a thick region of a Big Rock Point cladding thin foil specimen. (A) Selected area [denoted by the circle of (B)] diffraction pattern showing zone axes $[3\bar{2}\bar{1}\bar{3}]_{Zr_3O}$ // $[11\bar{4}\bar{7}\bar{6}]_{\alpha}$ and planes $(2\bar{1}\bar{2}3)_{Zr_3O}$ // $(10\bar{1}3)_{\alpha}$; (B) negative image of the dark-field morphology of the $(1i\bar{2}1)_{Zr_3O}$ reflection of (A).